Title	Evaluation of supercurrent distribution in High-TC superconductor by Scanning SQUID Microscopy
Author(s)	Sugimoto, Akira; Yamaguchi, Tetsuji; Iguchi, Ienari
Citation	Physica C: Superconductivity , 357-360 : 1473 - 1477
Issue Date	2001-08
DOI	10.1016/S0921-4534(01)00590-1
Self DOI	
URL	https://ir.lib.hiroshima-u.ac.jp/00046734
Right	Copyright (c) 2001 Elsevier Science B.V. This is not the published version. Please cite only the published version. この論文は出版社版でありません。引用の際には出版社版をご確認ご利用ください。
Relation	

Evaluation of supercurrent distribution in High-T_C superconductor by Scanning SQUID Microscopy (SSM)

Akira Sugimoto [1], Tetsuji Yamaguchi, and Ienari Iguchi

Department of Physics and CREST-JST, Tokyo Institute of Technology, 2-12-1 Oh-okayama, Meguro-ku, Tokyo, 152-8551, JAPAN

Abstract

Scanning SQUID Microscope (SSM) is a powerful tool for observing small magnetic flux. It measures the z-component signal of flux density, but it is also available for observation of current distribution by inverting the Biot-Savart law. We report the two dimensional (2D) vector mapping of current distributions in high-T_C superconducting YBa$_2$Cu$_3$O$_{7-y}$ (YBCO) thin films obtained by converting magnetic-field data measured by SSM. The current distribution contains those from both transport supercurrent and vortex current. The transport supercurrent is found to flow mainly along the edge of a stripline. The results are in good qualitative agreement with the calculated results based on simple London model. The YBCO films with an artificial grain boundary, i.e. Josephson boundary are also observed. The transport current seems to flows with avoiding the vortices, and an irregular vortex is observed at a point of grain boundary.

Introduction

Recently, the scanning SQUID microscope has been found to have very profitable application of superconductor for various purpose.[1][2] It has been pointed out that the SSM can also probe a current distribution by use of the inverted Biot-Savart's law, and the current distribution of a semiconductor chip at room temperature was reported by measuring the spatial distribution of magnetic field using an SSM.[2] The SSM has much advantage to compare with the other methods [4-6] in its sensitivity and it is suitable for the investigation of superconductors. The current and magnetic distributions of Josephson junction is interested subjects for application of Josephson devices and for basic understanding of superconductors because the vortex in a Josephson junction is strongly conected with the phase of order parameter in the junction. We report the supercurrent distributions of YBCO thin films with and without an artificial grain boundary. The observed magnetic signal was converted into the current distribution by the inverted Biot-Savart law and compared with the theoretical model.

Experimental and calculations

YBCO thin films were deposited by a pulsed laser deposition (PLD) method. The film thickness was about 100 nm. All samples were patterned by conventional photolithography technique and the Ar ion milling technique. The width of a YBCO stripline was about 100 μm. The critical temperature (T_C) was around 88 K and the critical current density (J_C) was about 10^7 A/cm^2 at 10 K.

The films with a grain boundary were deposited on the MgO bicrystal substrates (12 ° $\times$ 12 °) by PLD Method. The width of this YBCO stripline was about 40 μm.

The scanning SQUID microscope system (SII SQM2000) is almost similar to that of Ref. [7]. It contains a dc-SQUID magnetometer made of Nb/Al-AlO$_x$/Nb tunnel Josephson junctions combined with a one-turn pickup coil of 10 μm diameter. The sample-coil distance was less than 10 μm. A Cu wire coil was wound around the sample holder to generate a small magnetic field.

To obtain the current the two-dimensional vector distribution map from magnetic field data, we use the inverted Biot-Savart law. By assuming that the supercurrent in the specimen is limited to the sheet of film thickness d and the SQUID-sample separation distance z_0 is much larger than d ($z_0 \gg d$), the following formula can be applied. According to the work by Wikswo et al.[8], the inverted Biot-Savart's law in Fourier space in this case is given by

$$j_x(k_x, k_y) = -\frac{2i}{\mu_0 d}\frac{e^{kz_0}}{k}k_y b_z(k_x, k_y) \qquad (1)$$

$$j_y(k_x, k_y) = \frac{2i}{\mu_0 d}\frac{e^{kz_0}}{k}k_x b_z(k_x, k_y). \qquad (2)$$

where, b_z is 2D Fourier transform of magnetic field $B_z(x, y)$, j_x and j_y are Fourier transforms of current density $J_x(x, y)$ and $J_y(x, y)$, respectively, k_x and k_y are the spatial frequencies in x and y directions, $k = \sqrt{k_x^2 + k_y^2}$, μ_0 is the permeability of free space, i is the imaginary unit. J_x and J_y are obtained by inverse Fourier transformation of Eqs. (1) and (2).

---

[1]*E-mail address:* asugimoto@htsc.ap.titech.ac.jp

In practice, at first, the two-dimensional z-component of the magnetic field data from SSM are transformed into discrete FFT form, then j_x and j_y are calculated using Eqs. (1) and (2) in k-space, and finally, $J_x(x,y)$ and $J_y(x,y)$ are obtained by inverse FFT of $j_x(k_x, k_y)$ and $j_y(k_x, k_y)$.

Results and discussion

Figure 1 shows that the observed magnetic field images ((a) and (b)) and current distribution images ((A) and (B)) of YBCO thin film of 100 μm wide (y-direction) under different transport currents (1.0 mA in (a) and (A), 10 mA in (b) and (B)). The x-direction length of measured stripline was about 60 μm (A) and 25 μm (B), respectively. The current flows along the x-direction. In Fig. 1(a), the magnetic-field data contain a single trapped vortex, hence the current distribution consists of the sum of transport current and vortex shielding current. The transport current flows mainly along the edge of the stripline, and small circular current that generates the vortex is also seen in the center part of this image. By considering the spread of a magnetic field at the detecting position (about 10 μm height above the sample surface) and the pick-up coil of 10 μmϕ, the real vortex and transport currents would be localized in small area. Figures 2(a) and 2(b) show the
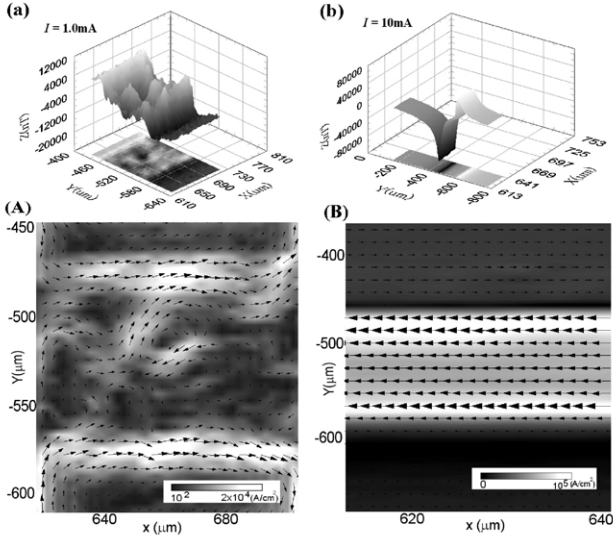

Figure 1: (a) Magnetic-field mapping of the YBCO thin film (100 μm width) in the presence of transport current (1.0 mA). (A) The calculated current distribution from Fig. 1(a). The length of each arrows indicate the magnitude of current density. (b) Observed magnetic-field mapping of the same sample as in Fig. 1(a) under different transport current (10 mA). (B) The calculated current distribution from Fig. 1(b).

magnetic-field data and the calculated current distribution across the film of Fig. 1(b) and 1(B) (at $x = 635$ μm), together with numerical results based on the sim-

ple London model, respectively. Since the transport current was only 1 % of film critical current ($\sim$1A), we assume the most ideal and classical model[9][10], $J(y) = I(a^2 - y^2)^{-1/2}/\pi$ in all but the extreme edge regions, where a is the half-width of stripline. The magnetic field is given by $B(y) = 0$ ($|y| < a$), $B(y) = \frac{\mu_0 I}{2\pi} y/(|y|\sqrt{y^2 - a^2})$ ($|y| > a$) . The calculated $B(y)$ and $J(y)$ profiles corre-
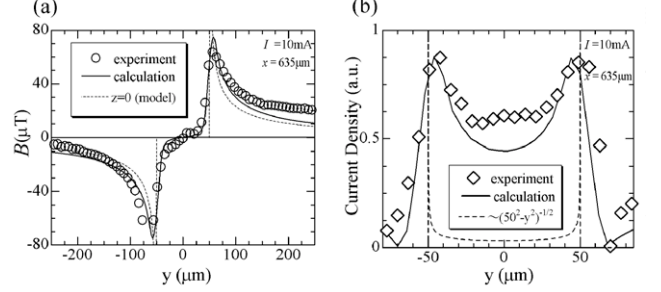

Figure 2: Comparison between the experimental data and the calculations for the magnetic and current profiles. The origin was set at the center of the stripline in each horizontal coordinate. (a) Open circle dots are the magnetic-field data across the film (x=635 μm) of Fig. 1(b). The dashed line is the sample surface ($z = 0$) distribution. The solid line is the calculated curve by assuming that the detection area of the pick-up loop and the SQUID-sample separation distance. (b) Open square dots are the experimental data of current density across the film of Fig. 1(B). The solid line is the calculated current distribution based on $B(x, y, z_0)$. The dashed line is the current distribution model on the surface.

spond to the dashed lines in Fig. 2(a) and 2(b), respectively. The solid line in Fig. 2(a) is the calculated result of a magnetic-field distribution at the detector position by assuming that the surface ($z = 0$) distribution given by this equation, $B(y)$ and $J(y)$. The open circle dots are experimental data. The agreement between the experimental data and the calculated result is qualitatively good. The solid line in Fig. 2(b) is the calculated current distribution based on $B(x, y, z_0)$. Open square dots are obtained from the experimental magnetic-field data in Fig. 2(a), and the dashed line is the current distribution model on the surface. The experimental current distribution almost agrees with the calculated result by taking the detection area of the SQUID loop into account. For 100 μm $< y <$ 200 μm, the discrepancy occurred due to the slight tilt of SQUID pickup coil to y-direction. Although the 2D mapping of current distribution does not exactly correspond to that of real surface ($z = 0$) itself, it essentially reflects the true nature of transport current or vortex current.

The current and magnetic distributions on the thin film with an artificial grain boundary are shown in Fig. 3. Fig. 3(a)-3(d) are the magnetic-field maps and 3(A)-3(D) are the calculated current maps with current vectors. This specimen was cooled down under a magnetic field of a few μT, then was measured at 3 K. Fig. 3(A), depicts

the initial state without transport current. Fig. 3(b) and 3(B) are under the presence of the transport current of 100 μA, Fig. 3(c) and 3(C) corresponds to 500 μA. The vertical dashed line of each figure corresponds to the artificial grain boundary in a bicrystal substrate. In Fig. 3(A), some circular vortex currents were seen. One downward direction vortex was clearly observed at the grain boundary interface. It is considered that the current might be perturbed by grains or some defects, hence irregular different direction vortex was generated. Such vortices were also seen in some YBCO thin films without artificial grain boundaries, however, they were more frequently observable in Josephson boundaries. In Fig. 3(B) and 3(C),
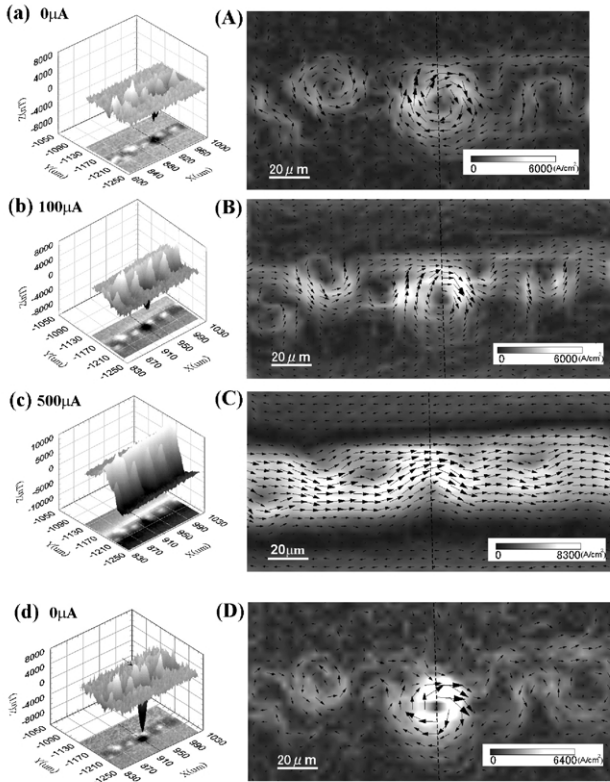

Figure 3:   Magnetic-field mappings ((a)-(d)) and calculated current mappings ((A)-(D)) of the YBCO thin film on a bicrystal substrate. (a) and (A) correspond to the case of the absence of transport current. (b) and (B) correspond to the case of transport current (100 μA), while (c) and (C) to the case of 500 μA. (d) and (D) are the results after supplying and cutting off the current exceeding Josephson critical current. Note that the measurement was done under the absence of transport current.

the transport current was found to flow with avoiding the vortices. The location of the vortices didn't change. Fig. 3(d) and 3(D) show the magnetic and current images after supplying and cutting off the transport current exceeding Josephson critical current, I_{JC}. At the grain boundary in Fig. 3(d), a new vortex was generated (indicated by arrow). The downward vortex was enhanced as compared

with that of Fig. 3(a). while the position of other vortices didn't change. It is explained that the current (higher than I_{JC} and lower than I_C (film itself)) makes super to normal transition only at the junction area. In this situation, the magnetic field induced by transport current was frozen in a moment when the current is reduced below I_C.

Summary

The 2D current distributions in YBCO thin films including an artificial grain boundary were obtained by SSM. In the 100 μm wide stripline of YBCO thin film, the transport current flows mainly at the edge of the stripline, and the agreement between the experimental data and the calculated results based on simple London model is qualitatively good. In the samples with the bicrystal Josephson junctions, one downward direction vortex was observed at the point of interface boundary. The transport current was found to flow with avoiding the vortices. The positions of vortices did not change for the transport current below the Josephson critical current, I_{JC}, but the generation of s a new vortex accompanying the enhancement of downward vortex component occured above the transport current of I_{JC}. It is considered that they might be caused by magnetic field induced by transport current at the interface boundary. These results demonstrate that the SSM system provides a useful tool for studying the current distribution in a superconductor.

References

[1] J. Dechert, M. Mueck, and C. Heiden, IEEE Trans. Appl. Supercond. 9, 4111 (1999).

[2] J. R. Kirtley, C. C. Tsuei, and K. A. Moler, Science 285, 1373 (1999).

[3] S. Chatraphorn, E. F. Fleetand, F. C. Wellstood, L. A. Knauss, and T. M. Eiles Appl. Pnys. Lett. 76 2304 (2000).

[4] Ch. Jooss, R. Warthmann, A. Forkl, and H. Kronmüller, Physica C 299, 215 (1998).

[5] P. D. Grant, M. W. Denhoff, W. Xing, P. Brown, S. Govorkov, J. C. Irwin, B. Heinrich, H. Zhou, A. A. Fife, and A. R. Cragg, Physica C 229 (1994).

[6] M. Tonouchi, M. Yamashita, and M. Hangyo J. Appl. Phys. 75 3387 (1999).

[7] T. Morooka, S. Nakayama, A. Odawara, and K. Chinone, Jap. J. Appl. Phys. 38, L119 (1999).

[8] B. J. Roth, N. G. Sepulveda, and J. P. Wikswo, Jr, J. Appl. Phys. 65, 361 (1989).

[9] E. H. Rhodeuck, and E. M. Wilson, Nature (London) 194, 1167 (1962).

[10] E. H. Brandt, Zeitschrift für Physik B 80, 167 (1990) (Eq. (30)).